Integrated Design and Control of a Flying Wing Using Nonsmooth Optimization Techniques

Yann Denieul, Joël Bordeneuve, Daniel Alazard,
Clément Toussaint, and Gilles Taquin

Abstract. In this paper we consider the problem of simultaneously stabilizing a civil flying wing aircraft and optimizing the control surfaces physical parameters, such as control surfaces sizes and actuators bandwidth. This flying wing configuration is characterized by unstable longitudinal modes, badly damped lateral modes, and a lack of control efficiency despite large movables. The question is then to determine the energy penalty associated to the control of these unstable modes, and more precisely to optimize the control surfaces architecture in order to minimize the control-associated energy. Our approach uses latest nonsmooth optimization techniques, which allows more possibilities on requirements specifications and controller structure compared to other approaches such as LMI-based optimizations. Results show a consistent behaviour for tuned parameters of the control surfaces.

1 Introduction and Motivation

Among other disruptive concepts for the future of civil aviation, the flying wing configuration has been studied for years [9]. This aircraft architecture combines several theoretical advantages compared to a "conventional" design. The main benefit provided by the flying wing concept is an enhanced aerodynamic efficiency, by eliminating all the devices (fuselage and tail planes) that do not create lift. As a result a better lift distribution along the span is achieved. The empty weight of

Yann Denieul · Joel Bordeneuve · Daniel Alazard
University of Toulouse-ISAE, 10, Av. Edouard Belin, 31055 Toulouse, France
e-mail: {yann.denieul,joel.bordeneuve,daniel.alazard}@isae.fr

Clément Toussaint
ONERA, 2, Av. Edouard Belin, 31055 Toulouse, France
e-mail: clement.toussaint@onera.fr

Gilles Taquin
Airbus Operations SAS, 316 route de Bayonne, 31060 Toulouse, France
e-mail: gilles.taquin@airbus.com

J. Bordeneuve-Guibé et al. (eds.), *Advances in Aerospace Guidance, Navigation and Control*, DOI: 10.1007/978-3-319-17518-8_27

the aircraft is also reduced, as is the overall wetted area. However this configuration faces some huge challenges which are yet to overcome. One of the main remaining challenge is the Handling Qualities resolution [13]. Indeed the flying wing has very special features that make it difficult to properly control and stabilize:

- No tailplane to trim the aircraft and damp the pitch oscillation.
- Forward aerodynamic center leading to a strong longitudinal instability.
- Control surfaces with poor pitch authority due to a weak longitudinal lever arm w.r.t. the center of gravity.
- Coupled control surfaces: trailing edge elevons are capable of providing pitching and rolling moments.
- Lack of lever arm of the vertical surfaces (if any) leading to a lack of yawing authority and a badly damped Dutch Roll mode.

Traditionnally, Aircraft Conceptual Design is concerned only with disciplines such as Aerodynamics, Performance, Weight and Handling Qualities. Control laws are designed afterwards, when the geometrical design is frozen. However for the flying wing case, such a sequential approach may be too restrictive: because of the previously mentioned specificities, active stabilization control laws are needed. A strong coupling exists between the plant — the flying wing— and the stabilizing controller; and it has been shown in [6] that such a coupling may lead to suboptimal design when the plant and controller are designed separately. The goal of our work is then (a) to identify potential physical limitations induced by the need for active stabilization and (b) to optimize the control architecture in order to minimize a physical criterion, e.g. energy needed to stabilize and control the aircraft.

This problem, known as *Plant-Controller Optimization*, *Co-design* or *Integrated Design and Control*, has been adressed in a variety of domains, such as Astronautics [2], Aeronautics [11], Chemistry [5] or Autonomous Underwater vehicles [15]. But whereas most of these studies have been using the Linear Matrix Inequalities (LMI) framework to solve the combined plant-controller optimization problem, the novelty of our approach is to use nonsmooth optimization techniques presented in [3]. Such a formulation allows for defining an arbitrary fixed-order controller, specifying physical parameters as controller parameters to be optimized and using a wider range of design specifications: constraints can be handled on the H_∞ form, but also as pole placement constraints. Moreover H_2 norm objectives can be taken into account.

This paper is organised as follows: in Section 2 the general model of the aircraft of interest is presented. In Section 3 the co-design optimization problem is set up. Then in Section 4 first results illustrating our approach are presented.

2 Problem Setup

In this section, the Flight Mechanics model of the Airbus Flying Wing model is presented. This paper only deals with longitudinal dynamics; however eventually both

longitudinal and lateral dynamics will be considered, for sizing cases concerning the elevons are multi-axes maneuvers.

2.1 Flight Dynamics Equations

The longitudinal Flight Mechanics equations can be written in the aerodynamic reference system $R_a(x_a, y_a, z_a)$ (see Figure 1):

$$m\dot{V} = -\frac{1}{2}\rho V^2 S C_D - mg\sin(\gamma) + F \tag{1}$$

$$-mV\dot{\gamma} = -\frac{1}{2}\rho V^2 S C_L + mg\cos(\gamma) \tag{2}$$

$$B\dot{q} = \frac{1}{2}\rho V^2 S l C_m \tag{3}$$

$$\theta = \alpha + \gamma \tag{4}$$

where:

- concerning aircraft parameters, m and B denote the aircraft mass and inertia around the y_a axis respectively, S and l are reference surface and length, corresponding to the wing aera and mean aerodynamic chord respectively.
- angles are classically defined as follows: γ, α and θ denote the flight path angle, angle of attack and aircraft pitch attitude respectively.
- concerning aerodynamic parameters, V denotes the aerodynamic speed, ρ denotes the air density, and C_D, C_L and C_m denote the drag, lift and pitching moment coefficients respectively.

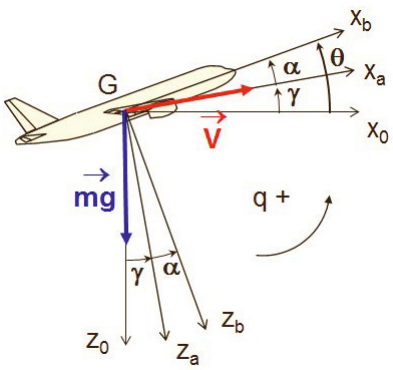

Fig. 1 Aerodynamic frame scheme.

Following classical assumptions on small angles approximations, this system of equations can be linearized and converted into the following state-space representation:

$$\begin{bmatrix} \delta\dot{V} \\ \delta\dot{\alpha} \\ \delta\dot{q} \\ \delta\dot{\theta} \end{bmatrix} = \begin{bmatrix} x_V & x_\alpha & x_q & x_\theta \\ -z_V & -z_\alpha & 1-z_q & 0 \\ 0 & m_\alpha & m_q & 0 \\ 0 & 0 & 1 & 0 \end{bmatrix} \begin{bmatrix} \delta V \\ \delta\alpha \\ \delta q \\ \delta\theta \end{bmatrix} + \begin{bmatrix} x_{\delta x} & x_{\delta m_i} \\ 0 & -z_{\delta m_i} \\ 0 & m_{\delta m_i} \\ 0 & 0 \end{bmatrix} \begin{bmatrix} \Delta\delta x \\ \Delta\delta m_i \end{bmatrix} \tag{5}$$

where the states are $\delta V, \delta\alpha, \delta q, \delta\theta$, which are the variations around an equilibrium of the airspeed, angle of attack, pitch rate, and attitude respectively. The different terms of the matrices are developped in the Appendix. Concerning the controls, $\Delta\delta x$ denotes the thrust command, and $\Delta\delta m_i$ denotes the i-th control surface command, the control surfaces architecture being developped in Section 2.2. In order to get the flight path angle γ as an output, and knowing the classical relation for longitudinal flight $\gamma = \theta - \alpha$, the output vector is chosen as follows:

$$\begin{bmatrix} \delta V \\ \delta\gamma \\ \delta\alpha \\ \delta q \end{bmatrix} = \begin{bmatrix} 1 & 0 & 0 & 0 \\ 0 & -1 & 0 & 1 \\ 0 & 1 & 0 & 0 \\ 0 & 0 & 1 & 0 \end{bmatrix} \begin{bmatrix} \delta V \\ \delta\alpha \\ \delta q \\ \delta\theta \end{bmatrix} \tag{6}$$

2.2 Control Surfaces Architecture

The control surfaces architecture deserves a special attention. The initial configuration of this flying wing includes five control surfaces on each side of the trailing edge. It has been demonstrated in previous studies [13] that in order to comply with maneuvrability specifications these surfaces should be multicontrol, i.e. elevons. Concerning yaw effectors, it has been shown [14] that control with crocodile flaps only is not satisfactory, and vertical surfaces are needed. The control surfaces general layout is visible on Figure 2. Using Figure 2 nomenclature, the general control vector is therefore: $u = [\Delta\delta x, LDQ1, \ldots LDQ5, RDQ1, \ldots RDQ5, LDR, RDR]'$, where $\Delta\delta x$ is the throttle command.

Now in the study presented here the two rudders are grouped as a single equivalent effector *DR*, for we are only concerned with longitudinal motion and control. Moreover in this paper we only deal with the control of the short period mode, as it will be explained in Section 2.3. Therefore we will not consider the throttle as a command. Including this control, for instance in order to design an autopilot for this aircraft, is a matter for future work. The final control vector considered in this study is finally: $u = [LDQ1, \ldots LDQ5, RDQ1, \ldots RDQ5, DR]'$. The control vector is eventually an 11^{th}-dimension vector.

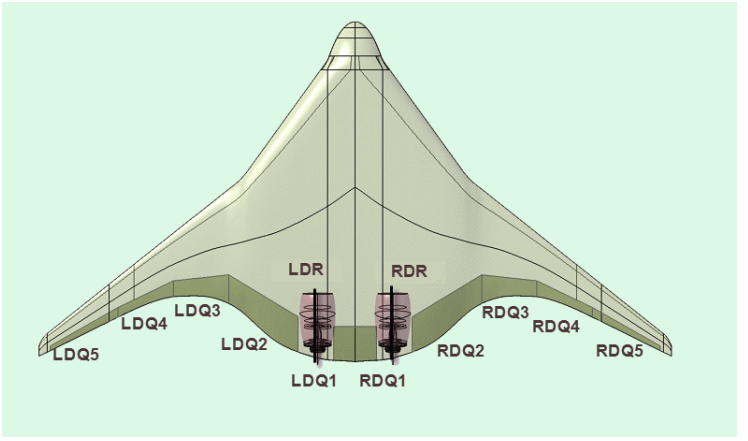

Fig. 2 Top view of the Airbus flying wing and its associated control surfaces architecture.

2.3 Longitudinal Dynamics Analysis

In this paper we focus on one particular challenge of this flying wing configuration: its longitudinal instability. Other issues, such as lateral instability, will be treated in a future work.

On an aircraft the x-wise relative position of the aerodynamic center w.r.t. the *CG* (center of gravity) is strongly linked to the aircraft longitudinal stability [18]. Now for aerodynamic planform optimization reasons, and due to the lack of any horizontal tail, on our flying wing configuration the aerodynamic center is located quite forward the *CG*. This leads to a consequent longitudinal instability, that needs to be controlled with active stabilization control laws.

Actually the short period mode leading to the longitudinal instability can be analyzed by extracting the $[\Delta\alpha, q]$ model from the state-space representation described in 2.1. The limit of stability associated to this subsystem occurs for a *CG* located at the so-called manoeuvre point, whose position is strongly linked to the aerodynamic center. A relative location of the manoeuvre point and *CG* can be found on Figure 3. The forward position of the manoeuvre point, especially in low speed, denotes a dynamic instability.

The poles of the complete longitudinal model are visible on Figure 4. The varying parameters are the aircraft mass, speed and altitude. The maximum unstable pole is obtained at low speed, light mass, and corresponds to a frequency of approximately 1.2 rad/s.

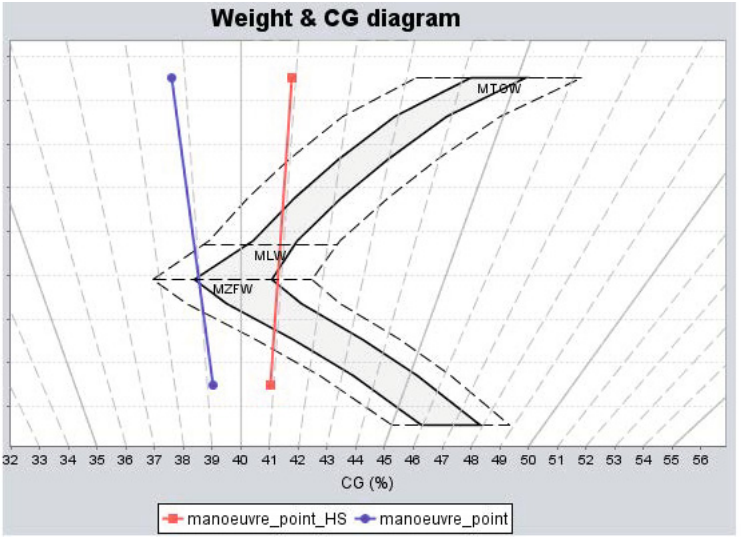

Fig. 3 Weight &*CG* diagram with manoeuvre point location for high and low speed.

3 Integrated Design and Control

In this section the general problem of integrated design and control is formulated. First the general equations are set in subsection 3.1, then this problem is adapted to our case in subsection 3.2.

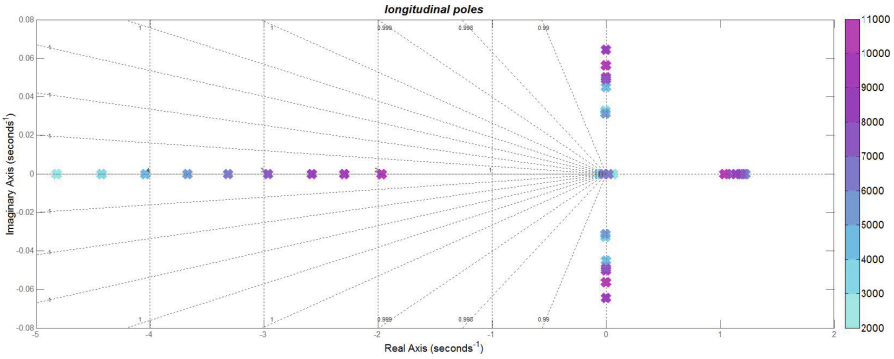

Fig. 4 Poles of the longitudinal model for M=0.55 and different altitudes. Altitude is given in meters. The complex conjugate poles correspond to the badly damped phugoid mode, which are easily controllable by an autopilot using the throttle command. The real modes correspond to the short period oscillation.

3.1 General Formulation

Following [6], the general combined plant / controller optimization problem is a multiobjective problem which can be stated on the form:

$$\begin{aligned} \min_{\xi,u(t),x(t),t_0,T} \max\{e(\xi), \Phi(x(t),T) + \int_{t_0}^{T} L(x(t),u(t),t)dt\} \\ \text{subject to : } h(\xi) = 0,\ g(\xi) \leq 0,\ \dot{x} = f(x(t),u(t),t,\xi), \\ \eta(u(t),t,\xi) \leq 0,\ \psi(x(t),t) = 0,\ x(t_0) = x_0 \end{aligned} \tag{7}$$

where ξ represents the physical parameters to be optimized, x are the states of the system to be controlled, u is the command vector.t_0 and T are the initial and final times, respectively.L is a controller cost functional. $h(\xi)$ and $g(\xi)$ represent respectively the equality and inequality constraints on physical parameters, Φ and ψ are final state objective and constraint respectively, and $e(\xi)$ is the objective function associated to the physical parameters. Finally η represents constraints on command vector. For an exhaustive description of the general optimal control problem formulation, please refer to [7].

3.2 Problem Specificities

In this section the previously described plant/controller optimization problem is adapted to our specific use-case.

- First of all for a fixed flight point and fixed physical parameters the state-space representation of the aircraft is supposed linear time-invariant with state feedback —indeed at this pre-sizing conceptual stage all the states are supposed known:

$$\begin{aligned} \dot{x}(t) &= A(\xi)x(t) + B(\xi)u(t) \\ y &= x \end{aligned} \tag{8}$$

- Moreover the structure of the compensator is restricted to a static state-feedback:

$$u = -Kx \tag{9}$$

- The cost function associated to the control objective is a linear quadratic, infinite-horizon criterion:

$$\min_{u(t)} J(u) = \frac{1}{2}\int_0^{+\infty} [x^T Q x + u^T R u]dt \tag{10}$$

  Such a criterion aims at minimizing the energy of the states x and of the control input u, weighted by two matrices Q and R respectively.
- Constraints on physical variables are of the form:

$$\forall i \in [1; n_{param}],\ \xi_{i_{min}} \leq \xi_i \leq \xi_{i_{max}} \tag{11}$$

$$\sum_{i=1}^{n_{param}} c_i \xi_i = C \tag{12}$$

For instance, if physical parameters include control surfaces sizes, constraints on these parameters would be that the total span of the control surfaces should not exceed the aircraft total span. In the example described in this paper such constraints will include bounds on the actuators bandwidth (see Equation 17). Indeed we are focusing in this work on an actuator bandwidth optimization, however future work will also include control surfaces sizing.

- Following previous work on integrated aircraft/controller design [11], constraints on control law performance are specified as follows:
  - Closed-loop stability.
  - Sufficient stability margins.
  - Adequate Handling Qualities performance. This may include sufficient stability, and appropriate maneuverability in order to comply with certification maneuvers.

To our knowledge, most plant/ controller optimizations applied to aerospace problems in the past years have been using the LMI framework [12] [19][8] [16]. In this approach all handling qualities constraints are cast as H_∞-norms of a transfer functions, e.g. $\|W^{-1}(s)T_{w\to z}\| \leq 1$ means that the closed-loop transfer $T_{w\to z}$ fits the frequency domain template $W^{-1}(s)$. The main interest of this approach lies in the fact that when correctly translated into an LMI formulation, the problem can be convexified and solved through dedicated LMI solvers.

However such a formulation quite differs from usual specifications used by engineers for defining acceptable handling qualities. Most of the time these specifications are expressed in terms of modes characteristics, such as minimal damping or frequency. Moreover controllers found by LMI solvers are unstructured and full-order. This means that these controllers have a n-th order internal dynamics, n being the order of the plant to control. This is not acceptable for our problem, for aircraft closed-loop characteristics should be obtained at the conceptual design stage with rather simple controllers, such as pitch and yaw dampers.

Therefore we propose a different approach: solve the plant/controller problem through nonsmooth optimization techniques for control synthesis developped in [4] and applied in [3]. This has two main advantages: on one side the possibility to tune fixed low-order controllers compliant with industrial applications and on the other side greater possibilities concerning closed-loop requirements. Two kinds of specifications available with these tools are of particular interest for our study: (a) the possibility to specify characteristics on closed-loop poles such as minimum damping, frequency or decay, and (b) the possibility to specify a multiobjective problem of the form H_2/H_∞. The H_∞ channel accounts for performance, and the H_2 channel minimizes the energy to control the aircraft. In the next section we will develop this approach and the first results it enables for co-design.

4 First Results

In this part the process we have set up is explained and first results are shown.

4.1 Control Problem Setup

According to the longitudinal model presented in 2.3, we focus on the flight point where the instability is maximal, corresponding to an unstable pole of frequency approximately 1.2 rad/s.

Following results presented in [1], we choose to set the H_∞ problem as a weighting on the acceleration sensitivity function. A disturbance w acts on the pitch acceleration $\dot{q}$. The desired behaviour for this acceleration is specified through a weighting function of the form $W_1 = \frac{s^2+2\xi\omega s+\omega^2}{s^2}$ with appropriate values of ξ and ω. The expected behaviour for $\dot{q}$ is therefore of the second-order form, and the shape of desired disturbance rejection profile on the acceleration W_1^{-1} is plotted on Figure 5.

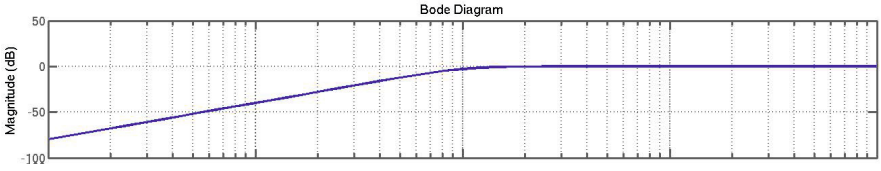

Fig. 5 Desired disturbance rejection profile on pitch acceleration W_1^{-1}.

The non-detectable double integrators $\frac{1}{s^2}$ of the weight W_1 can be removed by computing a minimal realization of the whole standard form.

The H_2/H_∞ problem is then set as follows: the H_∞ constraint is $\|T_{w\to z_{inf}}\|_\infty \leq \gamma_\infty$, with γ_∞ being a value slightly above 1; in practice we will assume $\gamma_\infty = 1.5$. z_{inf} is the output channel defined on Figure 6. This physically means that a sinusoidal perturbation of any frequency on the pitch acceleration shall not perturbate the closed-loop acceleration of a factor more than γ_∞. This channel shapes the pitch acceleration desired closed-loop behaviour. Then a minimization of the energy used to control the aircraft is performed through minimizing the following objective function: $\|T_{w\to u}\|_2$. This problem setup is depicted on Figure 6. Finally the controller is assumed to be a state-feedback static compensator such as: $u = -Kx$ with $x = [\alpha\ q\ \theta]^T$. K is therefore a 11×3 matrix, for there are 11 controls (see Section 2.2).

The initial control problem may then be written of the form:

$$\min_K \quad \|T_{w\to u}\|_2 \tag{13}$$

$$\text{subject to:} \quad \|T_{w\to z_{inf}}\|_\infty \leq \gamma \tag{14}$$

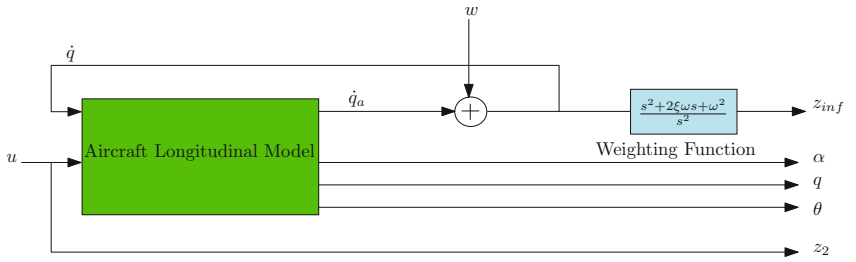

Fig. 6 H_2/H_∞ problem standard form with aircraft model (green) and weighting function (blue).

4.2 Implementation of the Co-design Problem

Now that the initial control problem is well defined, let us introduce some meaningful physical variables which should be optimized conjointly with the controller in order to solve the control problem. The underlying question is: how far is it possible to control our aircraft, and at which expense on the control system? A good rule of thumb, which may be found in [17], states that the actuators bandwidth to control the system should be at least ten times above the fastest mode. We aim at a more precise condition, and finally we should be able to evaluate the gains or penalties of considering an unstable aircraft configuration at a conceptual design phase.

In this paper we introduce actuators dynamics as first-order low-pass filters, which bandwidths are design parameters. More precisely, the 11 actuators blocks are modelled as follows:

$$\frac{y_{act}}{u_{act}}(s) = \frac{\omega_i}{\omega_i + s},\ i = 1...11 \tag{15}$$

where y_{act} and u_{act} are the actuators outputs and inputs respectively, as defined on Figure 7. $\Omega = [\omega_1, \dots \omega_{11}]^T$ is the vector of design parameters. In order to minimize these bandwidths (one needs the actuators to be as slow as possible: fast actuators mean high required energy, heavier and bigge actuators), a cost function is also added to the previous problem. An H_2-norm of the derivative of the actuators outputs is chosen: $\|T_{u_{act} \to \dot{y}_{act}}\|_2$. In the future a more physically meaningful function, such as the effectors kinematic energy, could be chosen.

The previously described control problem then becomes:

$$\min_{K,\Omega} \max\ \{W_2 \|T_{w \to u}\|_2, W_3 \|T_{u_{act} \to \dot{y}_{act}}\|_2\} \tag{16}$$

$$\text{subject to:}\ \ \|T_{w \to z_{inf}}\|_\infty \leq \gamma,\ 0 \leq \Omega \leq \Omega_{max} \tag{17}$$

where W_2 and W_3 are weightings associated to each objective function, and $0 \leq \Omega \leq \Omega_{max}$, which should be understood element-wise, specifies bounds on the actuators bandwidths. This problem has $3 \times 11 + 11 = 44$ variables.

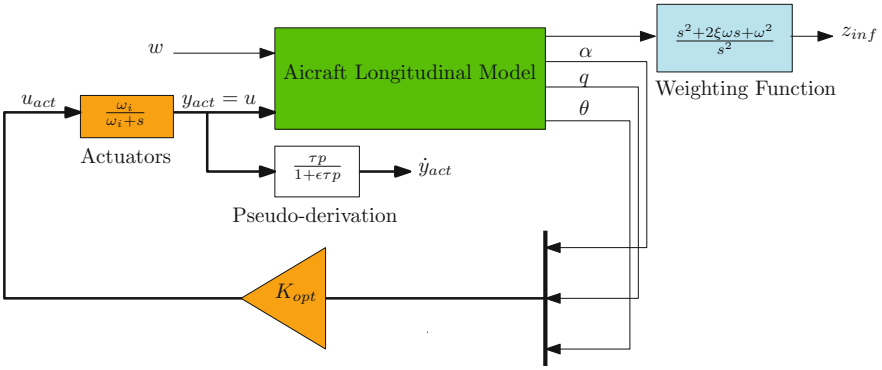

Fig. 7 Closed-loop problem for co-design approach. Tunable blocks are coloured in orange.

From an implementation point of view, it has been chosen to work with the `systune` and `slTunable` [10] routines for several reasons:

- It allows for mixed H_2/H_∞ synthesis and multiobjective optimization.
- It allows for structured parameters, such as fixed-order controllers and first-orders filters, which is appreciable for our problem. Moreover bounds on the variables are easily applicable.
- The `slTunable` syntax allows for directly specifying the closed-loop structure, as well as the tunable blocks and their structure. Moreover it allows dealing with a single `Simulink` model for synthesis and simulation, as it is performed on Figure 7.
- The constraints specifications are not limited to specifications on frequencies, but may also handle pole placement constraints. This may be more suitable to Handling Qualities purpose and will be adressed in a future work.

4.3 First Co-design Results

In this section the first results of the co-design approach are presented. A first synthesis is performed with variable bandwidths initialized to 20 rad/s, as well as with random initializations. The upper bound on the bandwidths is chosen to be also at 50 rad/s. The following controller is obtained (corresponding physical channels are shown as a reminder):

$$
K_{opt} = \begin{array}{ccc|l}
0.5816 & 1.1211 & 6.0981 & LDQ1 \\
1.3919 & 2.2578 & 14.5759 & LDQ2 \\
1.0279 & 1.7584 & 10.5422 & LDQ3 \\
0.9229 & 1.6367 & 10.0334 & LDQ4 \\
0.2329 & 0.3630 & 1.5500 & LDQ5 \\
0.5824 & 1.1203 & 6.0976 & RDQ1 \\
1.3904 & 2.2612 & 14.5797 & RDQ2 \\
1.0262 & 1.7594 & 10.5529 & RDQ3 \\
0.9235 & 1.6349 & 10.0309 & RDQ4 \\
0.2287 & 0.3664 & 1.5525 & RDQ5 \\
-0.0017 & 0.0028 & 0.0021 & DR \\
\hline
\alpha & q & \theta &
\end{array}
$$

At first sight, this controller looks rather consistent for:

- All pairs of elevons are commanded symmetrically (1 with 6, 2 with 7, etc), which seems obvious for a longitudinal kinematics, but which had not been specified as a particular structure for the controller.
- Gains have the right signs: for instance, for a positive $\delta\alpha$, one needs to deflect the elevons downwards, therefore positively.
- Magnitude of the gains follows elevons respective efficiencies. For instance, the second elevon has the largest surface, and it can be shown (see Figure 9) that it has the largest longitudinal efficiency. Therefore the controller chooses to use it accordingly.
- The rudder — last row — is set to almost zero.

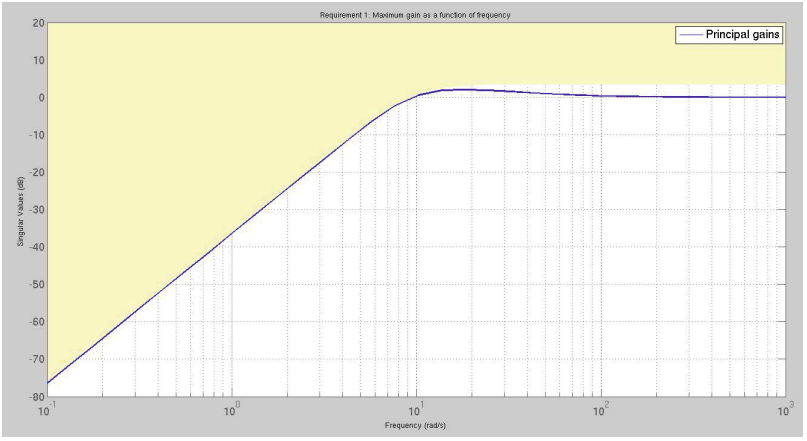

Fig. 8 Frequency-domain response of $T_{w\to z_{inf}}(K_{opt})$ (blue) and W_1^{-1} (coloured)

The optimal H_2 control objective is $\|T_{w\to u}\|_2 = 1.38$. As a comparison the optimal value given by an LQ synthesis for minimum energy control and infinite actuator bandwidth is 0.6, and the mixed H_2/H_∞ problem with also infinite actuator

bandwidth gives 1.26. Therefore adding actuators dynamics only slightly increase the objective. The closed-loop sensitivity function frequency response w.r.t. the desired weighting function is visible on Figure 8.

Then the actuators bandwidth, which are also tunable parameters, are also tuned in an interesting way. In order to meet the requirements, most bandwidths tend to be increased, however different bandwidths are allocated to the different control surfaces. The results can be found on Figure 9.

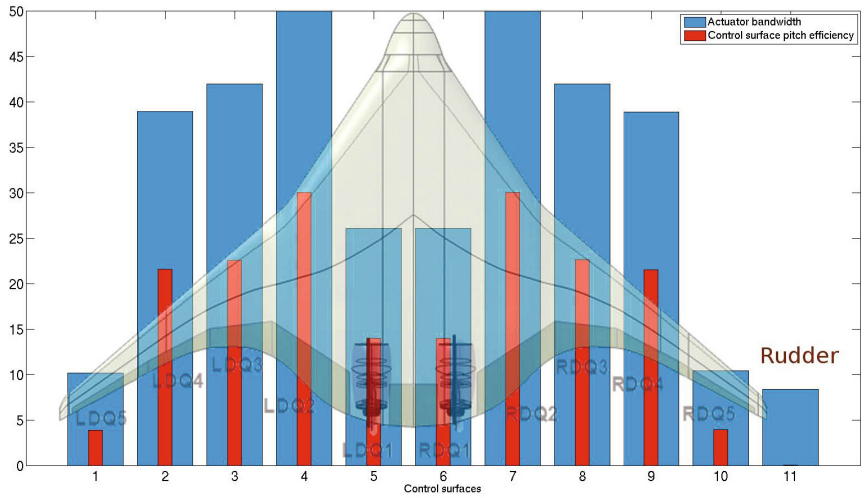

Fig. 9 Actuators tuned bandwidths (blue) and elevons pitch efficiencies (red).

Similarly to what was found for controller gains, bandwidths are tuned symetrically for symetrical elevons, which is physically consistent for longitudinal motion. Then the optimizer tends to use in a more powerful way — thus allocating more bandwidth— control surfaces that are the most efficient in creating pitching rate. For comparison purpose we plotted on Figure 9 control surfaces pitch efficiencies, corresponding to the the pitch rate row in the control matrix B. Finally for the most effective elevon —the second one, which is also the largest one— the upper bound of 50 rad/s is achieved; that tends to indicate that meeting the requirements is challenging on this configuration.

To conclude this part, it should be mentioned that here all actuators bandwidths were set as free variables and their symetrical tuning was checked afterwards only for method validation purpose. Symetrical results tend to indicate a consistent behaviour of the optimization. However, as in reality identical actuators are expected for symetrical control surfaces, further work should impose this constraint instead of expecting it as an output. As a result the complexity of the problem would be reduced.

5 Conclusion and Perspectives

In this work, a new method to integrated design and control is proposed. This method relies on nonsmooth optimizations techniques, and is applied to an unstable civil flying wing for longitudinal control. A mixed H_2/H_∞ synthesis is performed and actuators bandwidths are tuned simultaneously. This approach appears to be promising for conceptual aircraft design because of the diversity of criteria it may handle, and the fast calculations it allows. Future work may include different kinds of requirements, such as pole placement constraints, which is more suitable to handling qualities requirements. Then more "physical" objective functions, such as energy or mass minimization, should be handled. Also commonality of actuators for identical control surfaces will be imposed, hence leading to a simplification of the problem without loosing physical sense. Then future *co-design* will include not only actuators bandwidth as variables, but also physical control surfaces parameters such as their relative span along the trailing edge. Finally, this approach will be applied to longitudinal and lateral flight control co-design.

Acknowledgements. This work is part of a CIFRE PhD thesis in cooperation between ISAE and the Future Projects Office of Airbus Opérations SAS.

Appendix

Developping the elements of the state-space matrices gives:

$$
\begin{aligned}
x_V &= \tfrac{-\rho V S C_x}{m} + \tfrac{\partial F}{\partial V}, & x_\alpha &= -2gkC_{L_\alpha},\\
x_q &= \tfrac{-2gLk}{V} C_{L_q}, & x_\theta &= -g,\\
z_V &= \tfrac{-2g}{V^2}, & z_\alpha &= \frac{\rho V S}{2m} C_{L_\alpha},\\
z_q &= \tfrac{\rho S L}{2m} C_{L_q}, & m_\alpha &= \frac{\rho V^2 S}{B} C_{m_\alpha},\\
m_q &= \tfrac{\rho V S L^2}{2B} C_{m_q}, & x_{\delta x} &= \frac{1}{m}\frac{\partial F}{\partial \delta x},\\
x_{\delta m_i} &= -2gkC_{L_{\delta m_i}}, & z_{\delta m_i} &= \frac{\rho V S}{2m} C_{L_{\delta m_i}},\\
m_{\delta m_i} &= \tfrac{\rho V^2 S L}{2B} C_{m_{\delta m_i}}
\end{aligned}
$$

References

1. Alazard, D.: Reverse Engineering in Control Design. John Wiley & Sons (2013)
2. Alazard, D., Loquen, T., de Plinval, H., Cumer, C.: Avionics/control co-design for large flexible space structures. In: AIAA Guidance, Navigation, and Control (GNC) Conference, Guidance, Navigation, and Control and Co-located Conferences. American Institute of Aeronautics and Astronautics (2013), http://dx.doi.org/10.2514/6.2013-4638

3. Apkarian, P.: Tuning controllers against multiple design requirements. In: 2012 16th International Conference on System Theory, Control and Computing (ICSTCC), pp. 1–6. IEEE (2012)
4. Apkarian, P., Noll, D., Rondepierre, A., et al.: Nonsmooth optimization algorithm for mixed h2/h∞ synthesis. In: Proc. of the 46th IEEE Conference on Decision and Control, pp. 4110–4115 (2007)
5. Bansal, V., Ross, R., Perkins, J., Pistikopoulos, E.: The interactions of design and control: double-effect distillation. Journal of Process Control 10(2-3), 219–227 (2000)
6. Fathy, H., Reyer, J., Papalambros, P., Ulsov, A.: On the coupling between the plant and controller optimization problems, vol. 3, pp. 1864–1869 (2001)
7. Leitmann, G.: The calculus of variations and optimal control, vol. 24. Springer (1981)
8. Liao, F., Lum, K.Y., Wang, J.L.: An LMI-based optimization approach for integrated plant/output-feedback controller design. In: Proceedings of the 2005 American Control Conference, pp. 4880–4885. IEEE (2005)
9. Liebeck, R.: Design of the blended-wing body subsonic transport. 2005-06. von Karman Institute for Fluid Dynamics (2005)
10. MATLAB: version 2013a. Robust Control Toolbox. The MathWorks Inc., Natick, Massachusetts, USA (2013)
11. Niewhoener, R.J., Kaminer, I.: Linear matrix inequalities in integrated aircraft/controller design. In: Proceedings of the 1995 American Control Conference, vol. 1, pp. 177–181. IEEE (1995)
12. Niewoehner, R., Kaminer, I.: Integrated aircraft-controller design using linear matrix inequalities. Journal of Guidance, Control, and Dynamics 19(2), 445–452 (1996)
13. Saucez, M.: Handling qualities of the airbus flying wing resolution. PhD thesis, ISAE-Airbus, Toulouse (2013)
14. Saucez, M., Boiffier, J.L.: Optimization of engine failure on a flying wing configuration. AIAA, Minneapolis (2012)
15. Silvestre, C., Pascoal, A., Kaminer, I., Healey, A.: Plant/controller optimization with applications to integrated surface sizing and feedback controller design for autonomous underwater vehicles (AUVs) (1998)
16. Sridharan, S., Echols, J.A., Rodriguez, A.A., Mondal, K.: Integrated design and control of hypersonic vehicles. In: American Control Conference (ACC), pp. 1371–1376. IEEE (2014)
17. Stein, G.: The practical, physical (and sometimes dangerous) consequences of control must be respected, and the underlying principles must be clearly and well taught. IEEE Control Systems Magazine 272(1708/03) (2003)
18. Taquin, G.: Flight mechanics- master of science supaero (2009)
19. Yang, G.H., Lum, K.Y.: An optimization approach to integrated aircraft-controller design. In: Proceedings of the 2003 American Control Conference, vol. 2, pp. 1649–1654. IEEE (2003)